Selectivity Patterns in Alkane Oxidation over $Mg_3(VO_4)_2$–MgO, $Mg_2V_2O_7$, and $(VO)_2P_2O_7$

P. M. MICHALAKOS, M. C. KUNG, I. JAHAN, AND H. H. KUNG[1]

*Ipatieff Laboratory and Department of Chemical Engineering, Northwestern University,
Evanston, Illinois 60208-3120*

The catalytic oxidation of ethane, propane, 2-methylpropane, butane, pentane, and cyclohexane has been studied over $Mg_3(VO_4)_2$–MgO, $Mg_2V_2O_7$, and $(VO)_2P_2O_7$. These reactions produced a wide range of products ranging from alkenes, dienes, anhydrides, acids, and carbon oxides. Broadly speaking, the major products were dehydrogenation products over $Mg_3(VO_4)_2$, combustion products over $Mg_2V_2O_7$, and oxygen-containing organic products over $(VO)_2P_2O_7$, although there are exceptions to this broad generalization. From the product selectivities, the moles of oxygen consumed per mole of alkane reacted could be calculated. These were the average oxygen stoichiometries for the reactions. They had values of about unity for ethane oxidation over VPO, about two when oxidative dehydrogenation was the predominant reaction, and about four for the other reactions studied. The selectivity patterns in terms of the formation of dehydrogenation products versus oxygen-containing products including carbon oxides were explained by assuming that there existed a selectivity-determining step, which could be the reaction of the surface alkyl species or the adsorbed alkene before its desorption. The formation of oxygen-containing products would be facilitated if the surface alkyl or adsorbed alkene could interact with the vanadium ions in two adjacent VO_x units such that it could easily react with the reactive oxygen in the V–O–V bridge. The results of ethane oxidation, however, could not be explained simply by this model, and other factors needed to be considered. © 1993 Academic Press, Inc.

INTRODUCTION

It has always been intriguing to attempt to understand the selectivity patterns in catalytic oxidation of hydrocarbons. Over the years, various proposals have been forwarded to explain the changes in selectivities and yields for different reactions over various catalysts. A summary of these proposals can be found in various review articles and monographs (1–4). However, it is fair to say that none of the proposals is satisfactory in terms of being able to explain all available data. It is likely that because of the very different conditions under which the data were collected, the nature of the factors that determine selectivity is so different that it may range from the extent of secondary

reactions, to the relative rates of desorption of different products, to the probability of attack at various parts of a surface intermediate by reactive oxygen species.

From the studies of selective oxidation of light alkanes, it is apparent that the observed product distribution depends not only on the nature of the catalyst but also on the nature of the alkane (5–19). However, these reactions also share some common features. One of these features is that the breaking of the first C–H bond appears to be the rate-limiting step (10, 13). Another is that in the oxidation of butane over vanadates, the reducibility of the catalyst is important in determining selectivity for oxidative dehydrogenation: the more reducible the solid is, the less selective the catalyst is (20–22). This trend can also be interpreted in terms of the strength of the metal–oxygen bond: the weaker the metal–oxygen bond in the

226

solid is, the lower the selectivity is (23). However, this correlation does not appear to apply to the oxidative dehydrogenation of propane (18).

One would expect that if the nature and the reactions of the surface intermediate involved in the selectivity-determining step are known, the selectivity pattern can be understood. For example, if the oxidation of different light alkanes involves similar selectivity-determining steps, it is possible that the reducibility of the oxide could be a factor in determining selectivity in all these reactions. In this study, an attempt was made to identify the factors necessary to explain the selectivity data for different alkanes on three catalysts: $Mg_3(VO_4)_2$, $Mg_2V_2O_7$, and $(VO)_2P_2O_7$. The active sites in these vanadates are presumably made up of VO_x units bonded in different manners. This paper reports the result of this study.

EXPERIMENTAL

Catalyst Preparation

VPO—The catalyst was prepared by the recipe of Busca et al. (5). About 15 g of V_2O_5 (Aldrich 99.6+%) was refluxed for 3 h with constant stirring in a mixture of 60 mL of benzyl alcohol and 90 mL isobutyl alcohol. After stirring overnight at room temperature, 16.7 g of orthophosphoric acid crystals (Aldrich 99%) were added, and the solution was stirred at reflux for two hours followed by suction-filtering. The resulting rich, light-green powder was dried for 24 hours at 157°C. The catalyst was activated by heating to 400°C for 24 h in a flow of 2% butane, 21% oxygen, and the balance helium. X-ray diffraction patterns (XRD) were collected with a Rigaku Powder Diffractometer using Cu $K\alpha_{1,2}$ radiation with a Ni filter. The XRD of this sample showed only vanadyl pyrophosphate $((VO)_2P_2O_7)$ as the crystalline phase. The BET surface area was 28 m^2/g, and the bulk P/V ratio was 1.1 as determined by inductively coupled plasmon spectroscopy.

The VMgO catalyst was prepared as in (6) by adding a hot aqueous solution of

NH_4VO_3 to an appropriate amount of solid MgO. This slurry was concentrated into a thick paste by evaporation of excess water. After drying in air at 80°C, the resulting solid was crushed and calcined in air at 550°C for 6 h. The sample consisted of only two phases identifiable by XRD, $Mg_3(VO_4)_2$ and MgO, and its composition was determined by atomic absorption to be equivalent to 40 wt% V_2O_5 and 60 wt% MgO, and contained about 0.004 wt% K (7).

The $Mg_2V_2O_7$ was prepared as in (7) by adding an appropriate amount of aqueous ammonium metavanadate solution to MgO to result in a solid of 69 wt% V_2O_5 and 31 wt% MgO. The resulting slurry was dried, and the solid was ground and calcined in air at 550°C for 6 h. The XRD of this sample showed only the $Mg_2V_2O_7$ phase.

Reaction Studies

The activity and selectivity of the catalyst were measured in a fused silica microreactor. The temperature of the catalyst bed was monitored with a thermocouple in the center of the bed. The catalyst was supported by quartz wool, and the parts of the reactor before and after the catalyst bed were filled with quartz chips. Without a catalyst, there were no detectable conversions of hydrocarbons. For VPO, the steady-state reaction data was obtained using a feed of 2% hydrocarbon, 21% oxygen, and the balance helium. For both VMgO and $Mg_2V_2O_7$, the catalysts were pretreated in 60 mL/min oxygen for 1 h at 540°C before reaction. The reactant feed was 4% hydrocarbon, 8% oxygen, and 88% helium.

The products were analyzed by on-line gas chromatography using combinations of columns. For the pentane reaction over VPO, the analysis was performed with a VZ-7 column (Alltech, $\frac{1}{8}'' \times 20'$) for hydrocarbons and carbon dioxide, a 13X molecular sieve column ($\frac{1}{8}'' = 8'$) for carbon monoxide and oxygen, and a Porapak QS column ($\frac{1}{8}'' \times 15'$) for oxygenates including phthalic anhydride and maleic anhydride. The Porapak QS was used with

the following temperature program: 150°C for 5 min, 40°C/min to 190°C and held there for 10 min, then 30°C/min to 250°C and held there for 20 min. For the butane, propane, and 2-methylpropane reactions, a Graphpac GB column ($\frac{1}{8}'' \times 10'$) was used for analysis of oxygenates (maleic anhydride, acetic and acrylic acids) with the following temperature program: 2 min at 120°C, 15°/min to 190°C, and 14 min at 190°C. For the ethane reaction, Porapak Q was used to separate ethene and carbon dioxide. For all reactants except pentane, carbon monoxide and oxygen were separated by a Carbosphere column (Alltech, $\frac{1}{8}'' \times 6'$).

The conversion and selectivity were defined as

$$\text{Selectivity for product } P_i, S_i = \frac{y_i n_i}{\sum_i y_i n_i} \quad (1)$$

Conversion of alkane A, $X =$

$$\frac{\sum_i y_i n_i}{y_A n_A + \sum_i y_i n_i}, \quad (2)$$

where y_i and y_A are the mole fraction of product P_i and alkane A, respectively, n_i and n_A are the number of carbon atoms in each molecule of product P_i and alkane A, respectively, and all the terms were to be evaluated for the exit stream. The moles of O_2 consumed per mole of alkane feed, R_O, was calculated as

$$R_O$$
$$= \sum_i X S_i (O_2 \text{ stoichiometry to form } P_i). \quad (3)$$

The oxygen stoichiometries to form product P_i are listed in Table 1 for the products of interest here. It was assumed that in all of these reactions, any hydrogen not bound to the organic products would be present as water, and there was no molecular hydrogen in the product. Although the experimental setup was not equipped to detect water or hydrogen quantitatively, the validity of this assumption could still be tested by monitoring the oxygen conversion. This was performed for many experiments using the two

TABLE 1

Oxygen Stoichiometry in Reactions of Alkanes to Various Products

	O_2 consumed/ HC consumed
$C_2H_6 + 1/2O_2 \rightarrow C_2H_4 + H_2O$	0.5
$C_2H_6 + 7/2O_2 \rightarrow 2CO_2 + 3H_2O$	3.5
$C_3H_8 + 1/2O_2 \rightarrow C_3H_6 + H_2O$	0.5
$C_3H_8 + 2O_2 \rightarrow CH_2{=}CH{-}CHO + 2H_2O$	2.0
$C_3H_8 + 2O_2 \rightarrow 3/2CH_3COOH + H_2O$	2.0
$C_3H_8 + 5O_2 \rightarrow 3CO_2 + 4H_2O$	5.0
$C_4H_{10} + 1/2O_2 \rightarrow C_4H_8 + H_2O$	0.5
$C_4H_{10} + 3/2O_2 \rightarrow CH_2{=}C(CH_3)CHO + 2H_2O$	1.5
$C_4H_{10} + 5/2O_2 \rightarrow 2CH_3COOH + H_2O$	2.5
$C_4H_{10} + 7/2O_2 \rightarrow C_4H_2O_3{}^a + 4H_2O$	3.5
$C_4H_{10} + 13/2O_2 \rightarrow 4CO_2 + 5H_2O$	6.5
$C_5H_{12} + 1/2O_2 \rightarrow C_5H_{10} + H_2O$	0.5
$C_5H_{12} + 53/16O_2 \rightarrow 5/8C_8H_4O_3{}^b + 19/4H_2O$	3.3
$C_5H_{12} + 17/4O_2 \rightarrow 5/4C_4H_2O_3{}^a + 19/4H_2O$	4.25
$C_5H_{12} + 8O_2 \rightarrow 5CO_2 + 6H_2O$	8.0
$C_6H_{12}{}^c + 1/2O_2 \rightarrow C_6H_{10}{}^d + H_2O$	0.5
$C_6H_{12} + 3/2O_2 \rightarrow C_6H_6{}^e + 3H_2O$	1.5
$C_6H_{12} + 9O_2 \rightarrow 6CO_2 + 6H_2O$	9.0

^{a} Maleic anhydride.
^{b} Phthalic anhydride.
^{c} Cyclohexane.
^{d} Cyclohexene.
^{e} Benzene.

Mg vanadate catalysts. Within the relatively large uncertainties due to low oxygen conversions, the measured and calculated rates of oxygen agreed.

RESULTS

VPO

Some typical product distributions for the oxidation of C_2 to C_5 alkanes over the VPO catalyst are shown in Table 2. These data have been reproduced with at least two different preparations of the catalyst. In the test of each hydrocarbon, the catalyst was first activated as described in the Experimental section until a steady production of maleic anhydride was achieved before the reactant feed of the desired hydrocarbon was introduced. Thus the catalyst always started at the same state.

The VPO catalyst was quite selective for the oxidative dehydrogenation of ethane.

TABLE 2

Representative Product Distributions for Alkane Oxidation over V—P—O

Reactant	Reaction $T(^\circ C)$	W/F^a	$\%X^b$	%Selectivity[c]		
				CO	CO_2	C_2H_4
C_2H_6	305	5.3	2.4	12	7	81
	315	5.3	3.0	14	7	79
	325	5.3	3.9	15	7	78
	345	6.5	6.2	15	7	77
	335	5.3	6.0	19	6	75
	325	6.4	5.7	22	7	72
	350	6.4	8.0	26	7	67
	365	6.4	12	31	7	62
	375	8.3	16	38	8	54
	365	8.6	15	35	9	54
	385	8.3	22	45	8	47
	400	10.8	27	46	9	45
	425	5.4	27	46	9	45

				CO	CO_2	C_2H_4	C_3H_6	Ac	Ar		
C_3H_8	300	9.9	8.0	62	26	4	0	7	1		
	325	9.9	13	67	24	2	0	5	0		
	335	9.9	18	66	24	2	4	4	0		
	350	9.9	30	64	25	2	3	4	2		

				CO	CO_2	C_3H_6	Ac	Ar	Mthc	MA
2-methyl propane	275	10.2	6.5	34	27	1	28	1	1	8
	300	10.2	14	33	35	0	22	1	0	8
	325	10.2	26	31	40	0	18	1	0	9

				CO	CO_2	C_2H_4	C_3H_6	Ac	Ar	MA
C_4H_{10}	300	7.5	7.0	16	10	2	1	7	2	64
	325	7.5	17	19	14	2	1	6	1	60
	350	7.5	31	22	14	2	1	4	1	59
	375	7.5	49	25	13	1	1	1	1	58
	400	7.5	74	31	15	1	1	1	0	51

				CO	CO_2	MA	PA
C_5H_{12}	325	4.7	7.0	22	15	19	44
	325	9.5	14	21	12	27	39
	325	13.5	20	18	11	22	49

[a] Weight of catalyst/reactant flow rate, 10^4 g-min/mol alkane.
[b] % Conversion.
[c] AC = acetic acid, Ar = acrylic acid, MA = maleic anhydride, Mthc = methacrolein, PA = phthalic anhydride.

Ethene was the major product up to 22% conversion of ethane. Carbon oxides were the only other products, and no oxygenated organic compounds were detected. The selectivity for dehydrogenation decreased with increasing conversion. By comparing data obtained at different temperatures but about the same conversion, it was con-

cluded that the selectivity was much less a function of temperature than conversion. The selectivity to CO increased with increasing conversion, at the expense of ethene, whereas that for CO_2 increased only slightly.

The relatively high selectivity for oxidative dehydrogenation observed here for ethane differed from the results reported earlier in which carbon oxides accounted for over 90% of the products (8). It was not clear what caused the differences between the two investigations, since the catalysts appeared to behave similarly with other reactants. The reasons for the different observations were not investigated. A more recent paper using a VPO catalyst of a higher P/V ratio of 1.15 reported high selectivities for ethene at low conversions (17).

The oxidation of propane over this catalyst produced mostly carbon oxides. Less than 13% of the products were organic species, which comprised of propene, acetic and acrylic acids, and ethene. The selectivities for carbon oxides changed little in the range of low conversions. These results were similar to those reported earlier with only minor differences (8). In that report, carbon oxides accounted for over 90% of the products, and propene was the predominant selective product.

Similar to propane, the oxidation of 2-methylpropane also produced carbon oxides predominantly. However, there was a noticeably higher selectivity to acetic acid. Some maleic anhydride, but virtually no dehydrogenation products were detected. The appearance of maleic anhydride might be due to isomerization of 2-methylpropene, before its desorption, to butene followed by oxidation, since the surface of the VPO catalyst is acidic (12), and acid-catalyzed isomerization of this type is commonly known (24).

The product distribution for butane oxidation over VPO was similar to the literature reports (8, 13). The selectivity to maleic anhydride was at 60–64% up to 50% conversion, that for CO_2 was between 10 and 15%,
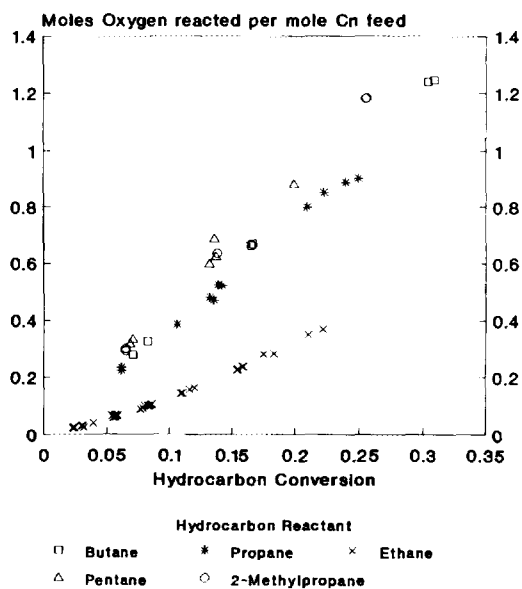

FIG. 1. The relationship between rates of oxygen consumption and alkane consumption for the VPO catalyst.

and small amounts of ethene, propene, and acrylic acid were also formed. There was a significant amount of acetic acid detected (4–7%) at less than 30% conversion, which decreased to 1% at higher conversions.

For pentane oxidation, phthalic anhydride and maleic anhydride were the main products, similar to observations reported in the literature (8, 12). The other products observed were CO and CO_2. No benzoic acid was detected. The selectivities for phthalic and maleic anhydride decreased at higher temperatures. The CO/CO_2 ratio was found to be around 1.5–1.7, while the literature result showed more CO_2 than CO (8, 12).

The moles of oxygen consumed per mole of alkane feed were calculated using eqn. (3), the stoichiometric numbers of Table 1, and the product distributions and conversions such as those shown in Table 2. These rates are plotted in Fig. 1 as a function of alkane conversion. They fall into two groups with the data for ethane in one group and the rest in another.

TABLE 3

Product Distributions for Alkane Oxidation over VMgO

Reactant	Reaction $T(°C)$	W/F^a	%Conv.	%Selectivity			
				CO	CO_2	C_2H_4	
C_2H_6	500	1.4	5.2	28	49	24	
	540	1.4	15	30	49	21	
	560	1.4	21	34	45	22	
				CO	CO_2	C_3H_6	
C_3H_8	500	0.6	8.4	14	24	62	
	500	1.2	16	17	31	52	
	540	1.2	25	20	30	48	
				CO	CO_2	$C_4H_8^b$	
2-methyl propane	475	0.27	4.0	6.9	22	71	
	500	0.38	8.0	10	26	64	
	500	0.53	12	14	33	53	
				CO	CO_2	$C_4H_8^c$	$C_4H_6^c$
C_4H_{10}	475	0.27	4.1	9	22	55	14
	500	0.36	7.5	11	22	49	19
	475	0.71	10	11	21	42	21
	500	0.60	15	11	24	39	24
	510	0.60	19	14	20	34	22
				CO	CO_2	$C_6H_{10}^b$	$C_6H_6^b$
$cC_6H_{12}^b$	484	0.14	8.4	3	14	47	36
	484	0.17	11	3	13	44	41
	484	0.51	21	4	15	27	54

^{a} Weight of catalyst/reaction flow rate, 10^3 g-min/mol alkane.
^{b} cC_6H_{12}: cyclohexane; C_6H_{10}: cyclohexene; C_6H_6: benzene, C_4H_8: 2-methylpropene.
^{c} Butenes and butadiene.

VMgO

Table 3 shows the representative product distributions for the oxidation of ethane (10), propane (9, 14), 2-methylpropane (10), butane (6, 10), and cyclohexane (11) over the VMgO catalyst taken from various reports. In general, dehydrogenation products were the dominant products, especially at low conversions, except in the oxidation of ethane. In the latter case combustion products dominated.

The moles of oxygen consumed per mole of alkane feed were plotted in Fig. 2 as a function of alkane conversion. The data for the different alkanes followed a common trend, including ethane in spite of its different selectivity for dehydrogenation.

$Mg_2V_2O_7$

The representative product distributions for ethane, propane, 2-methylpropane, and butane over $Mg_2V_2O_7$ are presented in Table 4. The data for propane, 2-methylpropane, and butane were taken from published re-

Moles Oxygen reacted per mol Cn feed

Hydrocarbon Conversion

Hydrocarbon Reactant

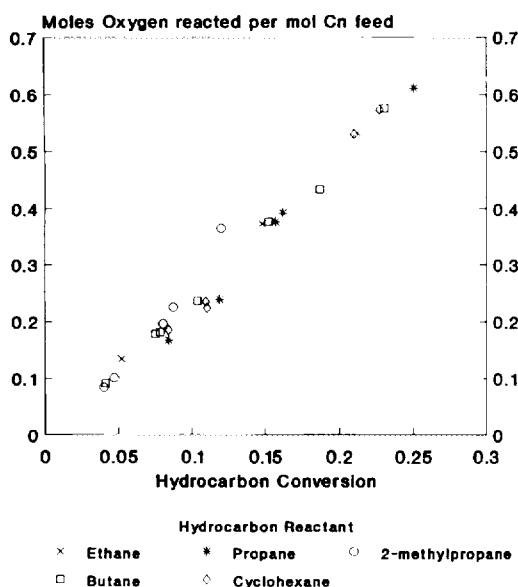| × Ethane	* Propane	○ 2-methylpropane
□ Butane	◇ Cyclohexane	

FIG. 2. The relationship between rates of oxygen consumption and alkane consumption for the VMgO catalyst.

ports (7, 10). Except with propane, where there was significant dehydrogenation, this catalyst produced mostly carbon oxides with these alkanes in the temperature range of 475–560°C.

The moles of oxygen consumed per mole of alkane feed are plotted in Fig. 3. The data followed two groups of behavior. Those for ethane and propane followed one group, and those for 2-methylpropane and butane followed another.

DISCUSSION

The results presented in Tables 2–4 clearly show that even for this limiting set of light alkanes, the selectivity depends on both the reactant and the catalyst, as one would expect. In particular, the types of selective oxidation products are very different on the different catalysts. For example, dehydrogenation products are the major selective products over the Mg vanadates. Very little oxygenates are produced. In contrast, oxygenates are the selective products

over VPO, and very little dehydrogenation products are formed, except in the case of ethane. This difference among the catalysts is not likely due to the difference in reaction temperatures. For example, at higher temperatures, VPO becomes much more of a combustion catalyst than a dehydrogenation catalyst (13).

In spite of the wide variations in the nature of products and selectivities, it is very interesting to observe that the moles of oxygen consumed and of hydrocarbon consumed show simple relationships (Figs. 1–3). Since the axes of these plots are relative rates of oxygen and alkane consumption, the slope of the line from the origin passing through each data point is the average number of oxygen molecules consumed per alkane molecule reacted to form that set of products, that is, the weighted average oxygen stoichiometry (AOS) for that set of products. If the reaction is highly selective and produces only one product, the slope of the line will be the same as the oxygen stoichiometry for the reaction to produce that product. The values of these oxygen stoichiometries are shown in Table 1. Thus for dehydrogenation products, the slope would be 0.5 for all alkanes. For total combustion to CO_2 and H_2O, the slope would range from 7/2 for ethane to 9 for cyclohexane. In general, the greater is the slope, the greater is the selectivity to oxygen-containing products.

The slopes of the lines from the origin passing through the data points increase with increasing conversion in all the plots. This is expected because the selectivity toward combustion products increases with increasing conversion due to secondary reactions such as combustion of selective oxidation products. Therefore, in order to simplify interpretation, only the data at low conversions (and the corresponding initial slopes of these plots) will be considered further. These initial slopes are the AOS for the formation of primary products and will be referred to as the initial AOS. Their val-

TABLE 4

Representative Product Distribution for Alkane Oxidation over $Mg_2V_2O_7$

Reactant	Reaction $T(°C)$	W/F^a	%Conv.	%Selectivity		
				CO	CO_2	C_2H_4
C_2H_6	540	6.3	3.2	49	21	30
	560	6.3	5.1	48	20	32
	571	6.3	6.5	53	22	25
				CO	CO_2	C_3H_6
C_3H_8	475	11.4	10	27	18	56
	500	11.4	16	33	21	46
	510	8.3	11	27	18	55
	540	8.3	13	26	20	54
				CO	CO_2	$C_4H_8^b$
2-methyl propane	502	3.6	6.8	39	36	25
	500	4.4	8.0	41	37	22
	540	3.6	11	44	38	17
				CO	CO_2	$C_4H_8^c$	$C_4H_6^c$
C_4H_{10}	500	3.7	6.8	33	33	31	3
	540	3.2	11	40	34	25	1
	503	9.0	18	44	39	15	2

^{a} Weight of catalyst/reacted flow rate, 10^3 g-min/mole alkane.

^{b} C_4H_8: 2-methylpropene.

^{c} C_4H_8: butenes; C_4H_6: butadiene.

ues are listed in Table 5 together with the predominant initial products.

There are a number of interesting observations illustrated in these tables and in Figs. 1–3:

(1) Table 5 shows that dehydrogenation products are the only predominant selective oxidation products over VMgO and $Mg_2V_2O_7$, whereas oxygen-containing organic products are the predominant selective oxidation products over VPO except in the case of ethane.

(2) The value of the initial AOS falls into three groups (Table 5). Its value is about unity for the oxidation of ethane on VPO, about two for all other reactions in which dehydrogenation is the predominant product, and about four for all other reactions

in which the principal products are either oxygen-containing organic molecules or combustion products.

(3) Ethane seems to behave differently from other alkanes on VMgO and VPO.

(4) The products from propane and 2-methylpropane are quite different on $Mg_2V_2O_7$. The principal reaction is dehydrogenation for propane but it is combustion for 2-methylpropane.

(5) Significantly more acetic acid is produced from 2-methylpropane on VPO than on $Mg_2V_2O_7$.

In the following, we will attempt to provide an explanation for these data.

General Assumptions

The data in this study were obtained with the three catalysts at near optimal condi-
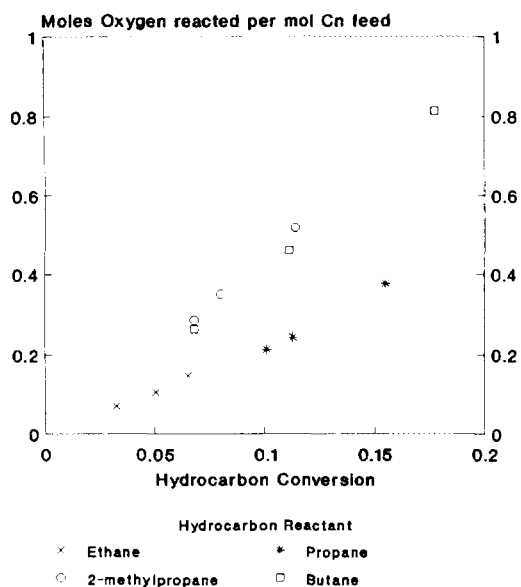
MICHALAKOS ET AL.

FIG. 3. The relationship between rates of oxygen consumption and alkane consumption for the $Mg_2V_2O_7$ catalyst.

tions in terms of selectivities. The selectivities at a particular conversion change only slightly with changing temperature or partial pressures of reactants. Centi and Trifiro reported that the activity of VPO in pentane oxidation as well as the product selectivity were similar for a feed of 21 or 33% oxygen (8). Likewise, the conversion of butane over VPO increased only slightly when the oxygen in the feed increased from 1–30%, while the selectivity to maleic anhydride was independent of the partial pressure of oxygen (25). A comparison of the data in this study with those in the literature (13, 25) also showed that the maleic anhydride selectivity at low butane conversions was little affected when the butane concentration in the feed was lowered from 2 to 1.1%, although a further decrease to 0.32% lowered the selectivity from 60 to 40%. The effects of oxygen partial pressure in the oxidation of ethane, propane, and 2-methylpropane over VPO were investigated in this study and the results are shown in Table 6. The data showed that the selectivities changed little with oxygen partial pressure. There was no change in the nature of the dominant products.

Published results also showed that on both the VMgO and the $Mg_2V_2O_7$ catalysts, changing the O_2/alkane ratio in the feed by a factor of four resulted in only small changes in the primary product distribution (7, 9). In particular, the nature of the pri-

TABLE 5

Summary of Number of VO_x Units in the Active Site the Molecule Readily Interacts with, Initial Average Oxygen Stoichiometry (AOS), and Characteristic Products

Catalyst	Reactant	No. of VO_x units accessible	Initial AOS	Predominant product
VPO	Ethane	1 (VO_5)	1.0 ± 0.04	Ethylene
	Propane	2	3.6 ± 0.1	CO
	2-Methylpropane	2	4.6 ± 0.1	CO
	Butane	2	4.0 ± 0.1	Maleic anhydride
	Pentane	2	4.6 ± 0.1	Maleic and phthalic anhydride
VMgO	Ethane	1 (VO_4)	2.5 ± 0.05	CO_2
	Propane	1	2.0 ± 0.05	Propene
	2-Methylpropane	1	2.1 ± 0.05	2-Methylpropene
	Butane	1	2.5 ± 0.05	Butenes
	Cyclohexane	1	2.1 ± 0.05	Cyclohexene
$Mg_2V_2O_7$	Ethane	1 (VO_4)	2.1 ± 0.05	CO
	Propane	1, 2 with difficulty	2.1 ± 0.05	Propene
	2-Methylpropane	1, 2 with difficulty	4.1 ± 0.1	CO_x
	Butane	2	3.9 ± 0.1	CO_x

TABLE 6

Effects of Partial Pressure of Oxygen on Activity and Selectivity for
Ethane, Propane, and 2-Methylpropane Oxidation over VPO

O_2/C_n Ratio[a]	Ethane		Propane		2-Methyl-propane	
	2	8	1.2	7	1.1	8
T (°C)	345	365	345	350	345	325
Conversion %	16	16	28	25	19	26
W/F^b (g min/ml)	0.17	0.16	0.16	0.12	(c)	
Selectivity %						
CO_2	8	9	26	25	38	31
CO	33	35	58	64	45	40
Ethene	58	56				
Acetic acid			5	4	4	18
Acrylic acid			3	2	2	1
Maleic anhydride			5	1	10	9

[a] Alkane concentration is kept at 2%.

[b] Wt. catalyst/total flow rate, g-min/ml.

[c] Comparison of activity is not being made for this case.

mary products remained the same. In addition, pulse reaction studies over VMgO (21) and VPO (26) using butane pulses without oxygen showed that the product selectivities in at least the first few pulses were similar to those in steady-state reactions. Thus these catalysts at steady state are in a nearly stoichiometric state. Furthermore, X-ray diffraction studies of catalysts after used in the oxidation of butane have established that the bulk phase of the crystals did not change. No new phases could be detected. Thus only the $(VO)_2P_2O_7$ phase was detected in the VPO catalyst (13, 27–29), only $Mg_3(VO_4)_2$ and MgO in the VMgO catalyst (6), and only $Mg_2V_2O_7$ in that catalyst (7).

In the following discussion, it is assumed that the exposed surfaces of the catalysts are represented by the low index crystal planes of $Mg_3(VO_4)_2$, $Mg_2V_2O_7$, and $(VO)_2P_2O_7$. In particular, it is assumed that the active sites of these catalysts involve VO_x units on the surface that are bonded in the same manner as in the bulk structures (30–32). Thus the active sites on $Mg_3(VO_4)_2$ are isolated VO_4 tetrahedra such that all the oxygen ions are bridged between a V and a Mg ion. For $Mg_2V_2O_7$, the active sites are

V_2O_7 units that can be viewed as pairs of corner-sharing VO_4 tetrahedra. A schematic drawing of these sites are shown in Fig. 4.

For the VPO catalyst, it is well established that a stoichiometric vanadyl pyrophosphate is somewhat less selective than one with a slight excess of phosphorus (13, 33). Furthermore, there appears to be an enrichment of phosphorus at the surface (13, 27, 34, 35). However, the exact nature of the excess phosphorus is still unknown. Since the emphasis of the discussion here is on the local bonding structure of the VO_x units, it will be assumed that the local structure of the active site is not affected by the excess phosphorus. In a highly selective catalyst, only the $(VO)_2P_2O_7$ phase has been detectable (13, 27–29). The average valence of vanadium in a VPO catalyst after use is about 4.1 (13, 27). This is consistent with the fact that vanadyl pyrophosphate is the major phase, and the mechanism proposed in the literature that the V ions in this catalyst undergo redox cycles (V(IV) $\leftrightarrows$ V(V)) during the reaction (13, 36, 37). Even when the catalyst is initially $VOPO_4$, it is slowly converted to vanadyl pyrophosphate in a reaction mixture (38). Since XPS investiga-
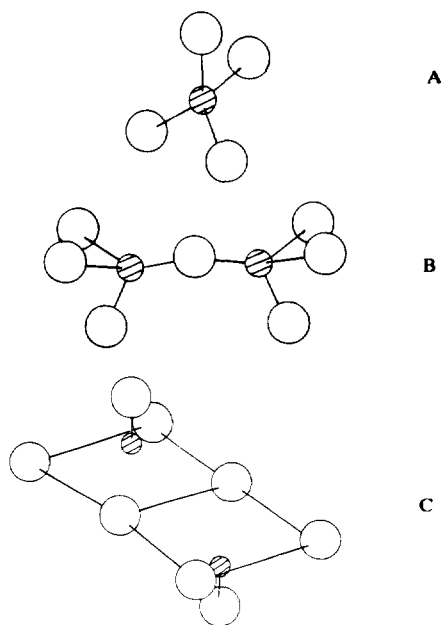
FIG. 4. Schematic drawing of the active sites: (A) VO_4 unit in $Mg_3(VO_4)_2$, (B) V_2O_7 unit in $Mg_2V_2O_7$, and (C) V_2O_8 unit in $(VO)_2P_2O_7$. Open circles are O ions and filled circles are V ions.

tion of used catalysts only detected small concentrations of V(V) on the surface, and V(V) on the surface of an air-calcined sample was converted to V(IV) after reaction (27, 35), we assume that most of the vanadium ions in the surface of a working catalyst is in the V(IV) state, and that the characteristic of the active site involved in the selectivity-determining step (to be discussed in detail later) can be represented by the V_2O_8 units made up of pairs of distorted edge-sharing VO_5 square pyramids found in $(VO)_2P_2O_7$ (28), as is shown in Fig. 4.

In this V_2O_8 unit, there is one V=O along the axial direction for each of the V ions. Opposite this V=O is a weak (long) V–O bond between V ions of different layers. For the present discussion, this weak bond is assumed to be inconsequential. There are also two oxygen ions bridging the two V ions in the V_2O_8 unit. These two oxygen ions are also bonded to phosphorus ions as they are the apex of the PO_4 units. There is no direct experimental evidence that identifies which of these oxygen ions participate in the redox cycle of an oxidation reaction. However, in the study of the oxidation of β-$(VO)_2P_2O_7$ to β-$VOPO_4$ using ^{18}O, it was established by following the peak shifts in the Raman spectra that the labeled oxygen is incorporated in the P–O–V bridging bond (39). Since there is direct evidence based on isotopic studies showing that bridging oxygen are involved in selective oxidation on molybdates (40), and bridging oxygen has been implied to be involved in other systems (6, 41), we will assume that the oxygen in the V–O–V bridge is involved in the reaction of the selectivity-determining step, although there are hypotheses that the vanadyl oxygen (V=O) is involved (42, 43).

It should be emphasized that the active sites under consideration are those involved in the step that determines selectivity (the nature of which is discussed later). It is possible that in steps subsequent to the selectivity-determining step, the surface species might react with other surface oxygen species in the active site or migrate to other active sites to complete the overall reaction.

The results of studies of deuterium isotope labeling and of effect of substituents on the reactivities of alkanes suggest that the rate-limiting step is the breaking of the first C–H bond (10, 26). It was observed here that at 500°C, the relative rates of reaction of propane : butane : 2-methylpropane were 1 : 1.3 : 1.9 over VMgO and 1 : 1.5 : 1.4 over $Mg_2V_2O_7$. The similarity of the relative rates over the two oxides suggests that the rate-determining steps on these catalysts are similar. Thus it will be assumed that for all the reactions considered here, the rate-limiting step is the breaking of the first C–H bond to form an adsorbed alkyl species.

Scope of Interpretation of Data

Although it would be very interesting to be able to explain the production of each product, the task is beyond our current understanding of the reactions, in spite of the fact that only primary products are being considered. To reduce the problem to a more manageable one, we use the initial

AOS values to classify the sets of products into two groups, excluding those from ethane: one set in which dehydrogenation products are dominant and for which the initial AOS values are about two, and another in which oxygen-containing products are dominant and for which the initial AOS values are about four. The latter includes both organic molecules and carbon oxides in the set.

With this classification, the simplified reaction scheme can be represented as:

alkane → alkyl → dehydrogenation products

$\searrow$ oxygen-containing products   (4)

[O] (oxygenates and CO_x).

An alkane molecule is first activated by breaking a C–H bond to form an alkyl species. This species can lose another hydrogen and desorb as a dehydrogenation product, or react with a surface lattice oxygen to form a C–O bond and eventually an oxygen-containing product. The reaction of the alkyl species is the selectivity-determining step under consideration. It should be noted that the same conclusions will result if we assume that the selectivity-determining step is the reaction of the adsorbed alkene. In that case, a dehydrogenation product is formed if the adsorbed alkene desorbs, and an oxygen-containing product is formed if it reacts further to form a C–O bond. Then the reaction of the adsorbed alkene is the selectivity-determining step:

desorb
alkane → adsorbed alkene ——→ dehydrogenation products

$\searrow$——→ oxygen-containing products   (5)

[O]   (oxygenates and CO_x).

We will attempt to explain the selectivity for the two sets of products. At low conversions, it is reasonable to assume that the reactions of the selectivity-determining step are irreversible. If this step is the reaction of an alkyl species, the chemical reactions may be represented as follows. Dehydrogenation products would be formed if the alkyl species reacts by breaking another C–H bond at the β-position:

$$M{-}O{-}M + *{-}CH_2{-}CH_2{-}R \rightarrow M{-}\overset{\overset{\textstyle H}{\textstyle |}}{O}{-}M + CH_2 = CHR + *. \qquad (6)$$

In this equation, * represents a surface ion in the adsorption site, and is assumed to be a V ion. Alternatively, if the alkyl species reacts not only by breaking a C–H bond, but also by forming a C–O bond, then an oxygen-containing product would be produced:

$$M{-}O{-}M + *{-}CH_2CH_2R + * \rightarrow M \overset{\overset{\textstyle HC{-}{-}{-}CH_2R}{\overset{\textstyle |}{\underset{\textstyle |}{\textstyle O}}}}{\square} M + * + *{-}H. \qquad (7)$$

If the selectivity-determining step is the re-action of the adsorbed alkene, the ∗–CH₂CH₂R species will be replaced by an adsorbed alkene.

Effect of Reducibility of Active Site

Since one branch of the selectivity-de-termining step involves the formation of a C–O bond, the reducibility of the active site may be an important factor. An inspection of the summary data in Table 5 shows that reactions that lead to high initial AOS occur on catalysts that have pairs of VO_x units as active sites, that is, V_2O_7 and V_2O_8 groups. In these active sites, there are oxygen ions bridging two easily reducible vanadium ions. These oxygen ions should be much more easily removed from the lattice than other oxygen ions. Thus these active sites can form C–O bonds easily, which would lead to the formation of oxygen-containing organic molecules or combustion products. In contrast, there are no oxygen ions bridg-ing two vanadium ions in $Mg_3(VO_4)_2$. Thus the lattice oxygen ions in this catalyst are much less reactive, and the tendency for this catalyst to form C–O bonds is lower, and dehydrogenation products are dominant on this catalyst.

That the ease of removal of lattice oxygen is an important factor in determining selec-tivity for oxidative dehydrogenation of bu-tane over vanadates has been demonstrated using orthovanadates of cations of different reduction potentials (22) and using sup-ported vanadia catalysts (23). This correla-tion of selectivity with the presence of reac-tive lattice oxygen fits most of the data in Table 5, but it does not explain the data for ethane or propane. To explain the data for propane, an additional factor of the effect of the size of the molecule compared to the active site is considered.

Effect of Size of Reactant Molecules

The selectivity-determining step involves the reaction of a surface alkyl species or an adsorbed alkene. The reaction between this species and the surface reactive lattice oxy-
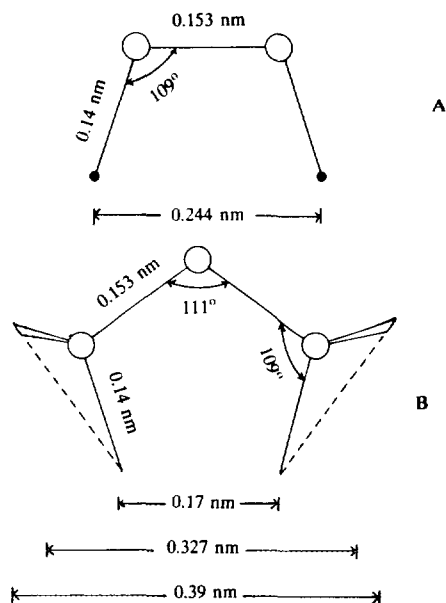

FIG. 5. Schematic drawing of geometry for (A) an ethyl species and (B) a propyl species.

gen is facilitated if the hydrocarbon interme-diate is bonded to both vanadium ions of the linked VO_x units such that the hydrocarbon species is being held close to the surface oxygen. This is possible only if the molecule is sufficiently large to do so. The separation of the vanadium ions in the active sites can be estimated from crystallographic data. For the V_2O_7 unit in $Mg_2V_2O_7$, the separa-tion is 0.339 nm (31); for the V_2O_8 unit $(VO)_2P_2O_7$, it is 0.319 nm (32). The separa-tion of V ions in adjacent VO_4 units in $Mg_3(VO_4)_2$ on a low index plane is 0.37 nm (30). Using a value of 0.072 nm for the ionic radius of V^{5+} (44) and a covalent radius of 0.07 nm for C (45), the V–C bond length is estimated to be 0.14 nm. Using this V–C bond distance, the V–V separation in an active site needed to bond with a surface C_2 and a C_3 species can be estimated (Fig. 5). From this, it can be seen that the C_3 species could readily bond with the two V ions in the active site of $(VO)_2P_2O_7$, but could do so only with difficulty with those in $Mg_2V_2O_7$. Based on this, one would argue that propane would react on $Mg_2V_2O_7$ as if the active sites

are isolated VO_4 units, like in $Mg_3(VO_4)_2$, whereas it would react like the larger hydrocarbons on $(VO)_2P_2O_7$. This is indeed observed. The exact nature of the C_3 species is not used in this geometric argument, although it could possibly be an allyl species. The schematic drawings in Fig. 5 also shows that the ethyl species is too small to interact with two V ions simultaneously in any of the three oxides.
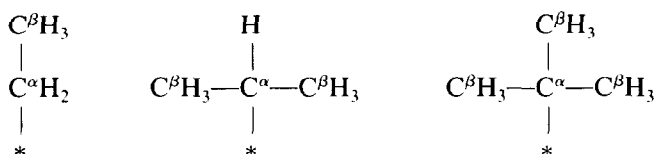
The manner in which a C_3 carbon chain bonds to the active site could explain the much larger production of acetic acid from 2-methylpropane than from propane on $(VO)_2P_2O_7$. From Fig. 5b, it can be seen that when a branched C_3 species bridges the adjacent VO_5 units in $(VO)_2P_2O_7$, the methyl group in the middle carbon is not interacting with the surface. This configuration is conducive to the formation of acetate group when the two carbon–carbon bonds of the C_3 unit are cleaved by reaction with the lattice oxygen. This explains the substantial production of acetic acid observed on this catalyst.

The difference between propane and 2-methylpropane on $Mg_2V_2O_7$ cannot be ex-plained by the size of the C_3 chain. We propose that although with difficulties, a C_3 species still has a finite probability to interact with both vanadium ions in a V_2O_7 unit to lead to the formation of combustion products. This probability is twice as large for 2-methylpropene than propane, which may account for the lower selectivity for dehydrogenation for 2-methylpropane on this catalyst.

Oxidation of Ethane

The behavior of ethane is different from the other alkanes. It is the only alkane that undergoes significant dehydrogenation on the VPO catalyst, as well as the only one for which combustion is the predominant reaction on VMgO. We offer a phenomenological explanation of this behavior. Since the active site on VMgO is an isolated VO_4 unit, various alkyl species should react in a similar manner. One can compare the possible reactions of ethyl, propyl, and 2-methylpropyl species statistically by counting the number of various types of bonds in each species:

$$
\begin{array}{ccc}
C^\beta H_3 & H & C^\beta H_3 \\
| & | & | \\
C^\alpha H_2 & C^\beta H_3-C^\alpha-C^\beta H_3 & C^\beta H_3-C^\alpha-C^\beta H_3 \\
| & | & | \\
* & * & *
\end{array}
$$

In these species, a reaction in which a C^β–H bond is broken would lead to dehydrogenation. However, breaking a C^α–H bond or cleaving a C^α–C^β bond would lead to degradation products. The statistical probability of these three processes is proportional to the number of these bonds in the species, which are shown in Table 7. They show that these species only differ in the relative number of C^β–H bonds. If the C^α–H and the C–C bond react with equal probability, whereas the C^β–H bond reacts somewhat faster, combustion would be more likely for ethane than for the other alkanes. Since the reaction conditions, especially temperatures, on the two Mg vanadates are similar, this argument about ethane should apply to Mg pyrovanadate also to account for the low dehydrogenation selectivity observed on this oxide.

For the VPO catalyst, for some unknown reasons, which may be related to the much lower reaction temperature, the C^β–H bond breaks much more readily than the C^α–H bond, and dehydrogenation becomes the dominant reaction. For the higher alkanes,

TABLE 7

Number of Various Types of Bonds in an Alkyl Species

Species	Number			Normalized value		
	C^β—H	C^α—H	C—C	C^β—H	C^α—H	C—C
Ethyl	3	2	1	6	4	2
Propyl	6	1	2	6	1	2
2-Methylpropyl	9	0	3	6	0	2

the formation of 1,3-diadsorbed species is very favorable that dehydrogenation is not an important reaction any more.

Oxygen-Containing Organic versus Combustion Products

The model presented above of the reaction of the surface alkyl species (or adsorbed alkene) in the selectivity-determining step does not distinguish the formation of oxygen-containing organic or combustion products. However, organic products are formed on VPO, whereas combustion products are formed on Mg vanadates. The difference may be due to the different tendencies of the lattice oxygen to either break a C–H bond and form a C–O bond or break a carbon–carbon bond (mostly likely a C=C bond) and form C–O bonds.

One possible difference is the temperature of reaction. The higher reaction temperatures over Mg vanadates favors combustion to oxygenate formation. Another possible difference could be the nature of the oxygen ions. Haber has proposed that nucleophilic oxygen tends to form C–O bonds only and electrophilic oxygen tends to break C=C bonds (46). In the stoichiometric compounds of Mg orthovanadate and Mg pyrovanadate, the V ions are in the +5 oxidation state, whereas in $(VP)_2P_2O_7$, the V ions are in the +4 state. Therefore, it is likely that the electron density of the oxygen ions in VPO is higher than in the Mg vanadates, and they are more nucleophilic. Thus the tendency for VPO to form oxygen-containing organic compounds is higher.

CONCLUSION

In this study, the selectivities in the oxidation of C_2 to C_6 alkanes were compared over three vanadate catalysts: $Mg_3(VO_4)_2$–MgO, $Mg_2V_2O_7$, and $(VO)_2P_2O_7$. The selectivities for dehydrogenation, formation of oxygen-containing organic products, and combustion depended on the hydrocarbon and the catalyst. The selectivity pattern can be explained assuming that the selectivity-determining step for all the reactions is either the reaction of the alkyl species or the adsorbed alkene. Except for ethane, the behavior of the alkanes can be understood by considering if the active site contains reactive lattice oxygen which are oxygen ions bridging two easily reducible vanadium cations, and if the size of the surface intermediate in this crucial step allows it to bond to both vanadium ions in the active site such that it can be readily attacked by the reactive lattice oxygen. The formation of oxygen-containing products, including carbon oxides, is the favored reaction if these conditions are met. Otherwise, dehydrogenation should be the predominant reaction. Such an interpretation makes use of the concept of site isolation and the effect of metal–oxygen bond strength on the selectivity (23, 47, 48). However, these general considerations need to be supplemented by other factors to explain the finer details of the results, including the reactions of ethane. They are insufficient to explain the formation of oxygen-containing organic products versus carbon oxides. To distinguish these products,

additional criteria and/or selectivity-determining steps are needed.

REFERENCES

1. Kung, H. H., *Ind. Eng. Chem. Prod. Res. Dev.* 25, 171 (1986); "Transition Metal Oxides: Surface Chemistry and Catalysis." Elsevier, Amsterdam, 1989.
2. Grasselli, R. K., and Burrington, J. D., *Ind. Eng. Chem. Prod. Res. Dev.* 23, 393 (1984).
3. Sokolovskii, V. D., *Catal. Rev.-Sci. Eng.* 32, 1 (1990).
4. Dadyburjor, D. B., Jewur, S. S., Ruckenstein, E., *Catal. Rev.-Sci. Eng.* 19, 293 (1979).
5. Busca, G., Centi, G., Trifiro, F., and Lorenzelli, V., *J. Phys. Chem.* 90, 1337 (1986).
6. Chaar, M., Patel, D., Kung, M., and Kung, H., *J. Catal.* 105, 483, (1987).
7. Kung, M. C., and Kung, H. H., *J. Catal.* 134, 688 (1992). The 44° 2θ peak reported in this reference for the XRD pattern of fresh $Mg_2V_2O_7$ was later found to be an artifact due to the spectrometer.
8. Centi, G., and Trifiro, F., *Catal. Today* 3, 151 (1988).
9. Chaar, M., Patel, D., and Kung, H., *J. Catal.* 109, 463 (1988).
10. Patel, D., Kung, M., and Kung, H., in "Proceedings, 9th International Congress on Catalysis, Calgary, 1988" (M. J. Phillips and M. Ternan, Eds.), Vol. 4, p. 1553. Chem. Institute of Canada, Ottawa, 1988.
11. Kung, M., and Kung, H., *J. Catal.* 128, 287 (1991).
12. Centi, G., Golinelli, G., and Busca, G., *J. Phys. Chem.* 94, 6813 (1990).
13. Centi, G., Trifiro, F., Ebner, J. R., and Franchetti, V. M., *Chem. Rev.* 88, 55 (1988).
14. Patel, D., Ph.D. Thesis, Northwestern University, 1988.
15. Oyama, S. T., and Somorjai, G. A., *J. Phys. Chem.* 94, 5022 (1990); Oyama, S. T., *J. Catal.* 128, 210 (1991).
16. Seshan, K., Swaan, H. M., Smit, R. H. H., van Ommen, J. G., and Ross, J. R. H., *Stud. Surf. Sci. Catal.* 55, 505 (1990).
17. Merzouki, M., Taouk, B., Tessier, L., Bordes, E., and Courtine, P., "10th International Congress on Catalysis, Budapest, 1992," paper O47, preprint.
18. Guerrero-Ruiz, A., Rodriguez-Ramos, I., Fierro,

J. L. G., Soenen, V., Hermann, J. M., and Volta, J. C., *Stud. Surf. Sci. Catal.* 72, 203 (1992).
19. Sam, D., Soenen, V., and Volta, J. C., *J. Catal.* 123, 417 (1990).
20. Patel, D., Andersen, P. J., and Kung, H. H., *J. Catal.* 125, 132 (1990).
21. Owen, O. S., Ph.D. Thesis, Northwestern University, 1991.
22. Owen, O. S., Kung, M. C., and Kung, H. H., *Catal. Lett.* 12, 45 (1992).
23. Andersen, P. J., and Kung, H. H., "Proceedings, 10th International Congress on Catalysis, Budapest, 1992," paper O4.
24. Pines, H., "Catalytic Conversion of Hydrocarbons." Academic Press, New York, 1981.
25. Centi, G., Fornasari, G., and Trifiro, F., *J. Catal.* 89, 44 (1984).
26. Pepera, M. A., Callahan, J. L., Desmond, M. J., Milberger, E. C., Blum, P. R., and Bremer, N. J., *J. Am. Chem. Soc.* 107, 4883 (1985).
27. Batis, N. Harrouch, Batis, H., Ghorbel, A., Vedrine, J. C., and Volta, J. C., *J. Catal.* 128, 248 (1991).
28. Johnson, J. W., Johnston, D. C., Jacobson, A. J., and Brody, J. F., *J. Am. Chem. Soc.* 106, 8123 (1984).
29. Contractor, R. M., Bergna, H. E., Horowitz, H. S., Blackstone, C. M., Malone, B., Torardi, C. C., Griffiths, B., Chowdry, U., and Sleight, A. W., *Catal. Today* 1, 49 (1987).
30. Krishnamachari, N., and Calvo, C., *Can. J. Chem.* 49, 1629 (1970).
31. Gopal, R., and Calvo, C., *Acta. Crystallogr. Sect. B* 30, 2491 (1974).
32. Gorbunova, Yu. E., and Linde, S. A., *Sov. Phys. Dokl.* 24, 138 (1979).
33. Wenig, R. W., and Schrader, G. L., *Ind. Eng. Chem. Fundam.* 25, 612 (1986).
34. Garbassi, F., Bart, J. C. J., Tassinari, R., Vlaic, G., and Lagarde, P., *J. Catal.* 98, 317 (1986).
35. Morishige, H., Tamaki, J., Teraoka, Y., Miura, N., and Yamazoe, N., *J. Chem. Soc. Jpn.* 113, 1983 (1989).
36. Cavani, F., Centi, G., Manenti, I., and Trifiro, F., *Ind. Eng. Chem. Prod. Res. Dev.* 24, 221 (1985).
37. Bordes, E., and Courtine, P., *J. Chem. Soc. Chem. Commun.*, 294 (1985).
38. Moser, T. P., and Schrader, G. L., *J. Catal.* 104, 99 (1987).
39. Lashier, M. E., and Schrader, G. L., *J. Catal.* 128, 113 (1991).
40. Glaser, L. C., Brazdil, J. C., Hazle, M. A., Mehicic, M., and Grasselli, R. K., *J. Chem. Soc. Faraday Trans. 1* 81, 2903 (1985).
41. Burrington, J. D., Kartisek, C. T., and Grasselli, R. K., *J. Catal.* 87, 363 (1984).
42. Busca, G., and Centi, G., *J. Am. Chem. Soc.* 111, 46 (1989).

43. Schiott, B., Jorgensen, K. A., Hoffmann, R., *J. Phys. Chem.* **95,** 2297 (1991).

44. Shannon, R., *Acta. Crystallogr. Sect. A* **32,** 751 (1976).

45. Atkins, P. W., "Physical Chemistry," 3rd ed. W. H. Freeman, New York, 1986.

46. Haber, J., *in* "Solid State Chemistry in Catalysis" (R. K. Grasselli and J. F. Brazdil, Eds.), Amer. Chem. Soc. Symp. Series, Vol. 279, p. 1. ACS, Washington, DC, 1985.

47. Callahan, J. L., and Grasselli, R. K., *AIChE J.* **9,** 755 (1963).

48. Morooka, Y., Morikawa, Y., and Ozaki, A., *J. Catal.* **7,** 23 (1967); Sachtler, W. M. H., Dorgelo, G. J. H., Fahrenfort, J., and Voorhoeve, R. J. H., *Rec. Trav. Chim. Pays.-Bas* **89,** 460 (1970).